The effect of reverted austenite in a selective laser melted Maraging 300 steel

F. Conde[1], J. Ávila[2], M. Oliveira[1]

[1]*Universidade de São Paulo, Departamento de Materiais, SP, Brazil*
[2]*Universidade Estadual de São Paulo, SP, Brazil*
E-mail: fabiofariaconde@gmail.com

Abstract

Additive manufacture is a principle of building products by addition of materials rather than subtraction. Maraging 300 is an ultra-high strength steel with significant alloy addition, resulting in a martensitic matrix and hardened by precipitation through ageing treatment. A maraging 300 was processed by selective laser melting and an investigation was carried out on mechanical properties and microstructural features.

A post heat treatment was applied aiming grain refinement and martensite-to-austenite reversion. Mechanical properties were evaluated after ageing by tensile test. Microstructure was assessed by SEM and TEM.

Keywords: Austenite reversion; Maraging 300; additive manufacture; selective laser melting; ductility improvement of 18Ni SLMed.

Introduction

Nowadays more flexible production is required from industries, with less material discard for higher sustainability. The upcoming additive manufacturing (AM) technology has found space in these demands.

AM produces objects by adding layer-by-layer out of a 3D CAD file [1]. AM has many different technologies and methods for the 3D build [2]. For metals, selective laser melting (SLM) is a very utilized technique, consisted of a bed powder fusion (PBF) process in which thermal energy selectively heats a specific region of the powder bed over-melting point [2]. Maraging steel metal powder has been largely employed in the study of a variety of AM technologies [3,4].

Usually AM parts presents slight increased strength but loss of ductility and toughness compared to its compared counterparts of conventional routes. Martensite-to-austenite reversion studies may act as a solution to poor ductility by improving strain-hardening ability, hardness by grain refinement and toughness [5–7] through the TRIP effect. Martensite-to-austenite reversion may be introduced by thermal cycling [8,9] or by isothermal tempering inside the $\alpha+\gamma$ diagram [10–12]

In this study, the SLMed maraging 300 steel was built and heat treated, erasing weld pool tracks and presenting a very fine microstructure. The aim of the present work is to study the effect of reverted austenite in a martensite matrix of a SLMed maraging 300 steel correlated to mechanical properties.

Experimental Procedure

The studied material was built via a SLM-PBF machine out of a maraging 300 powder. The final product is shown in Figure 1. Samples were subjected to heat treatment for mechanical properties

comparison. The studied conditions are described bellow as following in Table 1.

Figure 1. Selective laser melted specimens on substrate plate to be removed after build.

Table 1. Studied conditions of the SLMed maraging 300 and applied heat treatments.

Sample	Applied Heat Treatments	
	α-γ Reversion	Aging
S0	---	---
S1	---	480°C/3h
S2	610°C/30min	480°C/3h
S3	650°C/30min	480°C/3h

S0 was the as-built condition to serve as a comparative baseline. S1, the directed aged sample, the most common treatment for maraging fabricated by conventional routes. S2, sample with an intercritical isothermal tempering for martensite-to-austenite reversion, followed by aging. And S3, similar to S2, but tempered at 650 °C.

The material chemical composition was measured by optical emission analysis using an RL-4460 Thermo Fisher, and the carbon and sulfur contents were analyzed by a LECO CS844.

For microstructural assessment, samples were prepared according to ASTM E3 [13]. Samples were etched with 1 % HNO_3 ethanol solution for 10 seconds to reveal the microstructure. Light optical microscopy and Scanning electronic were utilized to obtain images of the respective microstructures. Also, transmission electronic microscope was used in few conditions to analyze reverted austenite morphology and formation features in the microstructure.

Rectangular samples of 60 mm in length were used to conduct tensile tests under the ASTM E8 [14] standard requirements. Tensile tests were conducted at room temperature, crosshead speed of 0.033 mm s^{-1} and a load cell with a maximum capacity of 100 kN.

The austenite content was measured via synchrotron beam light source for x-ray diffraction at the Brazilian National Synchrotron Light Source (LNLS). XRD measurements were performed spaced equally during the tempering of 610 °C and 650 °C. The in-situ tests involved the heating, soaking and cooling of samples using the X-Ray scattering and thermomechanical simulation experimental station known as XTMS. The beam energy used was 12 keV (corresponding to a wavelength of 1.033 Å).

Results and Discussion

Maraging product by SLM build was obtained with a chemical composition, according to Table 2.

Table 2. Chemical composition (wt. %) of maraging 300 alloy.

Ni	Co	Mo	Ti	Al	C	Fe
18.3	9.2	5.15	0.51	0.056	0.004	Bal.

Figure 2 shows the microstructural feature of the AB material, evidencing a typical weld pool tracks as well documented in the literature. In Figure 2a, weld pool tracks boundaries, and in Figure 2b, cellular and columnar morphology. Figure 3 shows the image of XRD from the 2D detector for the ran experiments.

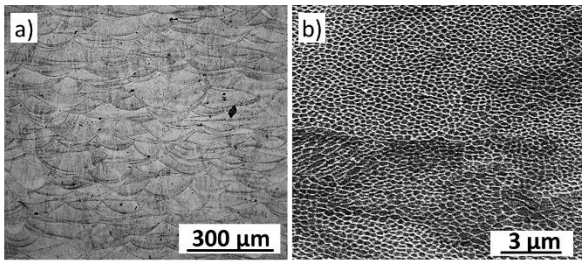

Figure 2. Images of the microstructural characterization of the as-built condition, a) light optical microscope image showing weld pool tracks; and b) scanning electronic microscope image showing the cellular microstructural array, typical of AM building procedure. Samples were etched with 1 % nitric acid + ethanol.

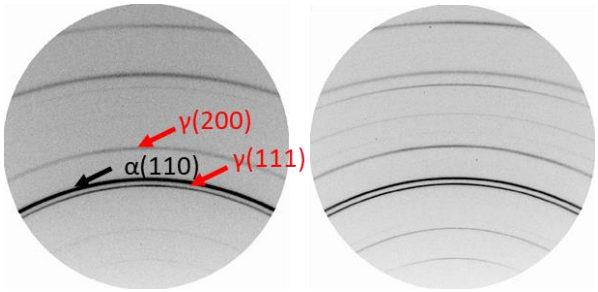

Figure 3. 2D diffraction pattern obtained in synchrotron analysis at LNLS. At left, heat treatment of a SLMed 18Ni at 610 °C temperature, at right, 650 °C.

Phase percentages were quantified using equations considering several crystal aspects and peak intensity, reported elsewhere [10]. For 650 °C, 80% of austenite was found in the end of treatment, with full thermal stability. For 610 °C, 44% of austenite was reverted.

The results from STEM analyses show the austenite phase and martensite after isothermal reversion treatment condition. In Figure 4 it can be seen that small islands of austenite start growing inside martensite, reaching significant size, and some islands remained small. Many formed at boundary and others inside martensite.

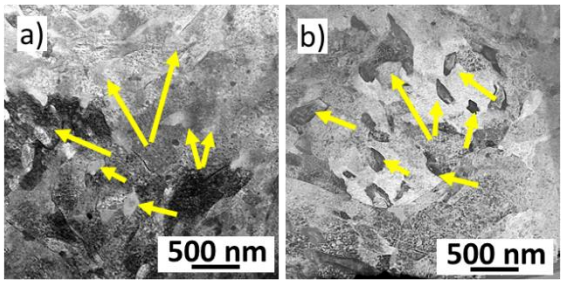

Figure 4. Scanning transmission electronic microscopy images analyses of SLMed 18Ni subjected to martensite-to-austenite reversion isothermal treatment. Yellow arrows indicating reverted austenite.

Table 3 depicts the results from tensile tests for mechanical strength evaluation. The highest tensile strength and lowest ductility were obtained for samples after direct aging at 480 °C/3h. As-built condition showed poor mechanical resistance and low ductility. Contrasting, samples subjected to martensite-to-austenite reversion treatments presented significant enhancement on ductility, however, at the expense of mechanical strength compared to the direct aged condition.

Table 3. Tensile tests results for mechanical strength and ductility assessment.

S	Yield Stress (MPa) [0,2%]	Tensile Strength (MPa)	E (mm)	γ_r (%)
S0	-	1246 ± 10	2.2 ± 0.1	0.2
S1	-	2112 ± 37	2.5 ± 0.3	0.5
S2	1411 ± 28	1440 ± 28	3.5 ± 0.1	44.0
S3	1165 ± 31	1375 ± 11	5.2 ± 0.3	80.1

Conclusions

• Reverted austenite can enhance ductility capacity with mechanical strength reduction.

• Martensite-to-austenite reversion may be triggered by isothermal heat treatment in the α+γ field.

• Direct aging provided the highest tensile strength and smallest ductility during test to rupture among treated samples.

References

[1] R. Singh, S. Singh, Additive Manufacturing: An Overview, Ref. Modul. Mater. Sci. Mater. Eng. (2017) 1–12. doi:10.1016/B978-0-12-803581-8.04165-5.

[2] ASTM F2792, F2792-12a - Standard Terminology for Additive Manufacturing Technologies, ASTM B. Stand. (2013) 10–12. doi:10.1520/F2792-12A.2.

[3] K. Kempen, L. Thijs, E. Yasa, J. Van Humbeeck, P. Procedia, E. Yasa, Microstructure and mechanical properties of Selective Laser Melted 18Ni300 steel Microstructure and mechanical properties of Selective Laser Melted, Phys. Procedia. 12 (2011) 255–263. doi:10.1016/j.phpro.2011.03.033.

[4] S. Hoeges, Development of a Maraging Steel Powder for Additive Manufacturing, Sinter Met. Eng. (n.d.).

[5] M. Wang, C.C. Tasan, D. Ponge, D. Raabe, Acta Materialia Spectral TRIP enables ductile 1 . 1 GPa martensite, Acta Mater. 111 (2016) 262–272. doi:10.1016/j.actamat.2016.03.070.

[6] D. Raabe, D. Ponge, O. Dmitrieva, B. Sander, Nanoprecipitate-hardened 1.5 GPa steels with unexpected high ductility, Scr. Mater. 60 (2009) 1141–1144. doi:10.1016/j.scriptamat.2009.02.062.

[7] M. Wang, C.C. Tasan, D. Ponge, A. Dippel, D. Raabe, ScienceDirect Nanolaminate transformation-induced plasticity – twinning-induced plasticity steel with dynamic strain partitioning and enhanced damage resistance, Acta Mater. 85 (2015) 216–228. doi:10.1016/j.actamat.2014.11.010.

[8] S.D. Antolovich, A. Saxena, G.R. Chanani, Increased Fracture Toughness in a 300 Grade Maraging Steel as a Result of Thermal Cycling, Metall. Trans. 5 (1974) 623–632.

[9] F.F. Conde, J.D. Escobar, J.P. Oliveira, M. Béreš, A.L. Jardini, W.W. Bose, J.A. Avila, Effect of thermal cycling and aging stages on the microstructure and bending strength of a selective laser melted 300-grade maraging steel, Mater. Sci. Eng. A. 758 (2019) 192–201. doi:10.1016/j.msea.2019.03.129.

[10] F.F. Conde, J.D. Escobar, J.P. Oliveira, A.L. Jardini, W.W. Bose Filho, J.A. Avila, Austenite reversion kinetics and stability during tempering of an additively manufactured maraging 300 steel, Addit. Manuf. 29 (2019) 100804. doi:10.1016/j.addma.2019.100804.

[11] J.D. Escobar, J.P. Oliveira, C.A.F. Salvador, G.A. Faria, J.D. Poplawsky, J. Rodriguez, P.R. Mei, S.S. Babu, A.J. Ramirez, Meta-equilibrium transition microstructure for maximum austenite stability and minimum hardness in a Ti-stabilized supermartensitic stainless steel, Mater. Des. 156 (2018) 609–621. doi:10.1016/j.matdes.2018.07.018.

[12] D. Raabe, S. Sandlöbes, J. Millán, D. Ponge, H. Assadi, M. Herbig, P.P. Choi, J. Milla, Segregation engineering enables nanoscale martensite to austenite phase transformation at grain boundaries: A pathway to ductile martensite, Acta Mater. 61 (2013) 6132–6152. doi:10.1016/j.actamat.2013.06.055.

[13] ASTM E3, E3-11 Standard Guide for Preparation of Metallographic Specimens 1, ASTM B. Stand. i (2011) 1–12. doi:10.1520/E0003-11.2.

[14] ASTM International, ASTM, ASTM E8 Standard Test Methods for Tension Testing of Metallic Materials, ASTM B. Stand. (2009) 1–27. doi:10.1520/E0008.